2013 European Control Conference (ECC)
July 17-19, 2013, Zürich, Switzerland.

Anti-windup Compensation for Electron Beam Stabilisation Control Systems on Synchrotrons with Rate Constrained Actuators

Sandira Gayadeen and Stephen Duncan

Abstract— **In modern synchrotron machines, electrons travelling at relativistic speeds in a closed circular path are bent by strong electromagnetic fields, which cause the electrons to lose energy in the form of synchrotron radiation. In order to achieve optimum performance, electron beam stability is a crucial parameter for modern synchrotrons. In particular, sub-micron stability is now a common requirement for the vertical position of the beam and to achieve the required performance, beam stabilisation feedback systems are used. A common nonlinearity encountered with the actuators in synchrotron feedback systems are the slew rate limits that are included in the circuits that apply power to the magnets in order to limit voltage changes. The large dimensions of synchrotron feedback systems and fast sample rates mean that robust Model Predictive Control (MPC) is not feasible. Therefore, for this application, anti-windup techniques for rate constrained nonlinearities are appropriate. The approach in this paper is anti-windup synthesis based on Internal Model Control (IMC) where it is demonstrated how IMC anti-windup synthesis for static constraints can be extended to rate constraints to improve constrained performance and guarantee stability. An Integral Quadratic Constraint (IQC) framework is used to analyse the robust stability of the system in the presence of both rate constraints and an infinity norm bounded uncertainty. Robust stability tests results and simulation of the anti-windup performance using machine data of the implementation of the control design on the Storage Ring of the UK's national synchrotron facility, Diamond Light Source are presented.**

I. Introduction

At synchrotron radiation facilities, electrons generated by an electron gun are accelerated until they reach their nominal energy ($\approx$ 3GeV for medium energy machines and $\approx$ 8GeV for high energy machines), and are transferred into a Storage Ring. Storage Rings consist of straight sections connected through a series of bends to form a closed loop. For example, the Storage Ring at Diamond, Oxfordshire, UK has 24 sections which create a ring of 561.6m in circumference [1]. Large bending magnets (dipoles) are used to curve the electron beam between adjacent straight sections and as the electron beam passes through a bending magnet, it emits a wide fan of synchrotron radiation that is channeled into a photon beamline. This synchrotron radiation spans the electromagnetic spectrum from infrared through visible and ultra-violet light to X-rays. The Storage Rings of modern synchrotron radiation facilities, such as Diamond, also use arrays of dipole magnets called Insertion Devices that cause the electron beam to oscillate along their length and so provide a tuneable source of synchrotron radiation by varying the magnetic field.

Although the position of the electron beam is maintained by the magnetic fields within the Storage Ring, the electron beam is subjected to disturbances from environmental effects that are coupled through the girders supporting the magnets. Several external disturbances cause electron beam perturbations, ranging from long-term disturbances, such as changes in air temperature during the day, to re-injections of the electron beam, which typically occur in the frequency range below 0.01Hz. Most disturbances arise from ground vibrations and residual effects after feedforward correction of Insertion Device field changes which lie within the range 0.01Hz and 100Hz [2]. Above 100Hz, the effects of vibration arising from cooling water pumps and girder cooling water flow resonances appear in the beam spectra [3].

Modern synchrotron radiation facilities are designed to produce high brilliance photon beams, which is achieved by emittance reduction in both planes. The vertical beam size defines the emittance which leads to requirements on the electron beam stability [2]. In order to achieve optimum performance, electron beam stability is a crucial parameter for modern light sources. In particular, sub-micron stability is now a common requirement for the vertical position of the electron beam. At Diamond, the electron beam must be controlled to within 10% of the beam size, which corresponds to an RMS variation less than 12.3μm in the horizontal plane and 0.6μm in the vertical plane [4]. To achieve such performance, beam stabilisation feedback systems are used. The feedback system uses electron beam position monitors (BPMs) to detect the electron beam position around the Storage Ring and calculate offsets to corrector magnet power supplies in both the horizontal and vertical directions.

In this paper, beam stabilisation systems are considered to be analogous to cross-directional processes, which are common in process industries such as paper machines, plastic film extrusion and metal rolling [5]–[9]. The term cross-directional describes systems where it is required to control variations of a measured variable in a profile that is orthogonal to the direction of propagation of the variable. A cross-directional control design approach is suitable for this application because there is considerable interaction between the spatial responses of each of the magnets and also because this spatial response is decoupled from the dynamic response of the actuators.

A common nonlinearity encountered with corrector magnets in synchrotron feedback systems is slew rate limiters

*This work was supported by Diamond Light Source Ltd.

The authors are with the Department of Engineering Science, University of Oxford, Parks Road, OX1 3PJ, Oxford, UK. {s.gayadeen,s.duncan}@eng.ox.ac.uk

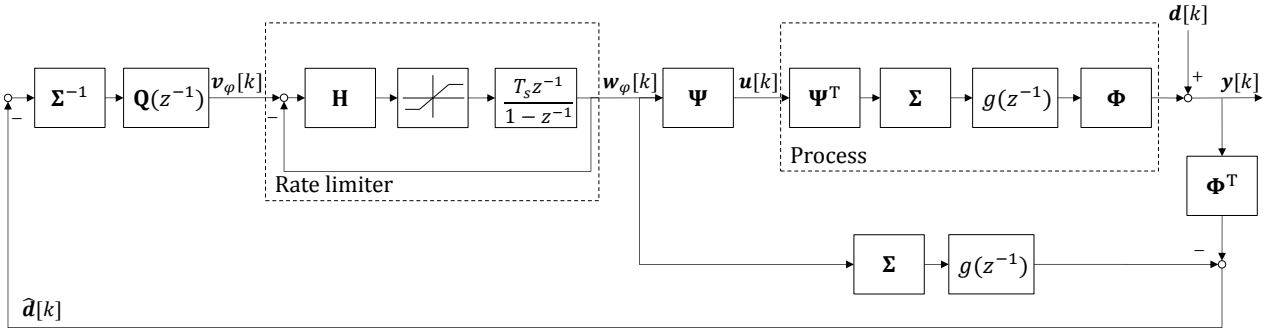

Fig. 1. Closed loop system with rate limiter in modal form

on the circuits in the power supplies for the corrector magnets due to voltage limitations [10]. The size of the control problem (172 actuators and sensors in both horizontal and vertical planes) and fast sample rate (10kHz) mean that robust constrained Model Predictive Control (MPC) is not feasible because of the computational burden. Anti-windup compensation is therefore an appropriate choice for rate constrained electron beam feedback systems with the aim of reducing the deviation between linear and nonlinear control signal rate. The anti-windup compensation within the Internal Model Control (IMC) structure described in [7], [11] is adopted in this paper. Standard IMC was not intended as an anti-windup scheme and therefore gives poor performance for saturating systems. Therefore a common anti-windup treatment in an IMC framework for saturating actuators is to modify the standard IMC structure to include a feedback term around the saturation [12]–[14]. Extending this approach to rate constraints has been mentioned in [14] where it is proposed that the design for static constraints can be applied to rate constraints by introducing a first-order filter after the non-linearity and thereby satisfying the rate constraints.

In this paper, the IMC anti-windup synthesis for rate limited actuators is considered in more detail. In particular, a specific rate limiter model is considered which represents the nonlinearity as a cascaded saturation function with an integrator and gain enclosed within a feedback loop [15], [16]. An Integral Quadratic Constraint (IQC) framework is used which models a general infinity norm-bounded plant uncertainty and the rate limiter to determine the robust stability of the system. This model matches the actual implementation at Diamond and is a common representation of rate limiters in aircraft applications [17], [18]. Anti-windup compensation within an IMC structure is then designed for rate limiters which, unlike saturations, already include an internal feedback path. Additionally, because this rate limit model is not L_2 stable, the approach in [19] is used to modify the rate limiter by including a first-order filter after the nonlinearity.

This paper is structured as follows. In Section II the model of the process and rate limiter are presented. In Section III the stability of the rate limiter is discussed and in section IV the IMC anti-windup design is presented. Section V demonstrates the use of IQCs to model the rate limiter and determine the system stability. Robust stability results of the Storage Ring system and simulation of machine data to determine the performance of the anti-windup compensation are presented as a case study in section VI. Conclusions are drawn in section VII.

II. Problem Formulation

The system under consideration is shown in Fig. 1. For synchrotron systems, the response is well approximated by,

$$\mathbf{y}[k] = g(z^{-1})\mathbf{B}\mathbf{u}[k] + \mathbf{d}[k] \tag{1}$$

where $\mathbf{d}[k]$ is an external disturbance, $\mathbf{u}[k] \in \mathbb{R}^N$ are the inputs to the N actuators and $\mathbf{y}[k] \in \mathbb{R}^M$ represents the deviation of the electron beam position for the ideal orbit in either horizontal or vertical directions measured at M sensors at times $\{t = kT_s : k \in \mathbb{Z}^+\}$, with T_s being the sample interval so that $\mathbf{y}[k] = \mathbf{y}(kT_s)$ [11]. The open loop dynamic response of the system is dominated by the first order response of the power supply units for the corrector magnets and the delay in the sensor data acquisition and processing, so that,

$$g(z^{-1}) = z^{-\nu}\frac{b_0 + b_1 z^{-1}}{1 - a_1 z^{-1}} \tag{2}$$

where ν is the smallest integer satisfying $\nu T_s > \tau$ and

$$\begin{aligned} a_1 &= e^{-aT_s} \\ b_0 &= 1 - e^{-a(T_s - \tau')} \\ b_1 &= e^{-a(T_s-\tau')} - e^{-aT_s} \end{aligned} \tag{3}$$

with a being the bandwidth of the actuator response (in rad.s^{-1}), τ being the delay in the system and $\tau' = \tau - (\nu - 1)T_s$.

The static response, represented by $\mathbf{B} \in \mathbb{R}^{M\times N}$, is a map from actuator to sensor position which captures the DC response of the actuators to a change in the transverse orbit position measured at mth sensor due to a transverse kick at the nth corrector magnet [20]. For $M \leq N$, the response matrix can be expressed in terms of reduced singular value decompositions such that,

$$\mathbf{B} = \mathbf{\Phi}[\mathbf{\Sigma} \quad \mathbf{0}]\begin{bmatrix}\mathbf{\Psi}_1^{\mathrm{T}} \\ \mathbf{\Psi}_2^{\mathrm{T}}\end{bmatrix} \tag{4}$$

where $\mathbf{\Phi} \in \mathbb{R}^{M\times M}$, $\mathbf{\Sigma} \in \mathbb{R}^{M\times M}$, $\mathbf{\Psi}_1 \in \mathbb{R}^{N\times M}$ and $\mathbf{\Psi}_2 \in \mathbb{R}^{N\times(N-M)}$. Defining $\boldsymbol{\eta}[k] = \mathbf{\Phi}^{\mathrm{T}}\mathbf{y}[k]$, $\mathbf{w}_\varphi[k] = \mathbf{\Psi}_1^{\mathrm{T}}\mathbf{u}[k]$ and $\boldsymbol{\mu}[k] = \mathbf{\Phi}^{\mathrm{T}}\mathbf{d}[k]$ projects the response into modal space so that for each mode,

$$\eta_m[k] = g(z^{-1})\sigma_m w_{\varphi_m}[k] + \mu_m[k] \tag{5}$$

Typically, the input signal $u_m[k]$ applied to each actuator is rate constrained such that

$$u_{rl}^{min} \le u_m[k] - u_m[k-1] \le u_{rl}^{max}. \tag{6}$$

However the rate constraints may be introduced to the controller with the condition,

$$u_{rl}^{min} + \left[\mathbf{\Psi}\mathbf{w}_\varphi[k-1]\right]_m \le \left[\mathbf{\Psi}\mathbf{w}_\varphi[k]\right]_m \le u_{rl}^{max} + \left[\mathbf{\Psi}\mathbf{w}_\varphi[k-1]\right]_m. \tag{7}$$

The rate limit nonlinearity is modeled as the feedback loop depicted in Fig. 1 [18] and is represented by the function $\varphi(.)$ where for each mode

$$\dot{w}_{\varphi_m}[k] = H\mathrm{sat}(v_{\varphi_m}[k] - w_{\varphi_m}[k]), \quad w_{\varphi_m}(0) = 0 \tag{8}$$

with sat(.) being a saturation function defined by

$$\mathrm{sat}(u_m[k]) = \begin{cases} u_m[k] & |u_m[k]| \le u_{sat} \\ u_{sat} \times \mathrm{sign}(u_m[k]) & |u_m[k]| > u_{sat} \end{cases} \tag{9}$$

where u_{sat} is the magnitude at which the input signal saturates. It is assumed that when the nonlinearity is not active, the system behaves linearly and the closed loop is asymptotically stable and well-posed. When the rate limits have not been reached (i.e. the saturation block in Fig. 1 acts as the identity) the model is defined by

$$\varphi(z^{-1}) = \frac{HT_s z^{-1}}{1 + (HT_s - 1)z^{-1}} \tag{10}$$

i.e. it behaves as a low pass filter with cut-off frequency determined by H. When the rate limits have been reached the rate limit model is interpreted as a restricted tracking problem [16].

III. Stability of the system

Due to the presence of the integrator term in the rate limiter model, which has a pole on the unit circle, the interconnection of the rate limiter is not L_2 stable, a condition which is required for analysis within the IQC framework [21]. In [19], this is resolved by connecting the rate limiter in series with a filter so that $\tilde{w}_{\varphi_m}[k] = \rho(z^{-1})w_{\varphi_m}[k]$ When no constraints are active, the modified nonlinearity becomes,

$$\tilde{\varphi}(z^{-1}) = \frac{HT_s z^{-1}}{1 + (HT_s - 1)z^{-1}}\rho(z^{-1}). \tag{11}$$

For the Diamond Storage Ring the gain H is chosen so that $H = 1/T_s$, therefore $\tilde{\varphi}(z^{-1})$ is,

$$\tilde{\varphi}(z^{-1}) = z^{-1}\rho(z^{-1}) \tag{12}$$

so for the analysis in this paper,

$$H = \frac{1}{T_s} \quad \text{and} \quad \rho(z^{-1}) = \frac{1}{z^{-1}}. \tag{13}$$

The L_2 stability of the modified rate limiter with this choice can be determined following from the analysis in [19].

Lemma 1 (L_2 stability of discrete rate limiter): For the rate limiter function $\tilde{\varphi}(z^{-1})$ in (12) and $\dot{\mathrm{sat}}(0) = K$ with $0 < K < \infty$, define Δ_φ as the system $v_{\varphi_m}[k] \to \tilde{w}_{\varphi_m}[k]$, where

$$\begin{aligned} \dot{w}_{\varphi_m}[k] &= \mathrm{sat}(v_{\varphi_m}[k] - w_{\varphi_m}[k]) \\ \tilde{w}_{\varphi_m}[k] &= w_{\varphi_m}[k] + \mathrm{sat}(v_{\varphi_m}[k] - w_{\varphi_m}[k]) \end{aligned} \tag{14}$$

and $w_{\varphi_m}(0) = 0$, the system is stable and the induced L_2 induced gain in the channel $v_{\varphi_m}[k] \to \tilde{w}_{\varphi_m}[k]$ does not exceed $\max\{\mathrm{K}, \sqrt{2}\}$ [19].

Proof: For the rate limiter shown in Fig. 1 with filter $\rho(z^{-1})$ connected to the output,

$$\begin{aligned} \dot{w}_{\varphi_m}[k] &= \mathrm{sat}(v_{\varphi_m}[k] - w_{\varphi_m}[k]) \\ \tilde{w}_{\varphi_m}[k] &= \rho(z^{-1})\frac{HT_s z^{-1}}{1 - z^{-1}}\dot{w}_{\varphi_m}[k]. \end{aligned} \tag{15}$$

For the Diamond rate limiter parameters in (13),

$$\tilde{w}_{\varphi_m}[k](1 - z^{-1}) = \mathrm{sat}(v_{\varphi_m}[k] - w_{\varphi_m}[k]). \tag{16}$$

Since $\tilde{w}_{\varphi_m}[k] = \rho(z^{-1})w_{\varphi_m}[k]$ then

$$\tilde{w}_{\varphi_m}[k] - w_{\varphi_m}[k] = \mathrm{sat}(v_{\varphi_m}[k] - w_{\varphi_m}[k]) \tag{17}$$

which corresponds to the case of $a = 1$ in [19]. It follows then that the induced L_2 gain in the channel $v_{\varphi_m}[k] \to \tilde{w}_{\varphi_m}[k]$ does not exceed $\max\{K, \sqrt{2}\}$. ■

IV. Controller Design

A. Unconstrained Design

Since the synchrotron uses an array of identical magnets to control the location of the beam, the actuators are assumed to have the same dynamics. Therefore individual modes can be controlled independently, so that $\mathbf{Q}(z^{-1})$ in Fig. 1 is

$$\mathbf{Q}(z^{-1}) = \mathrm{diag}\{q_m(z^{-1})\} \tag{18}$$

and the unconstrained system is described by

$$\begin{aligned} w_{\varphi_m}[k] &= -{\sigma_m}^{-1} q_m(z^{-1})\varphi(z^{-1})\hat{d}_m[k] \\ \hat{d}_m[k] &= \eta_m[k] - \sigma_m g(z^{-1}) w_{\varphi_m}[k]. \end{aligned} \tag{19}$$

From the stability analysis in Section III, a modified rate limiter is required for closed loop stability analysis. This means that the plant model must be adjusted to reflect the modified rate limiter, so a filter $\left[\rho(z^{-1})\right]^{-1}$ is introduced at the input to the plant such that

$$\tilde{g}(z^{-1}) = z^{-(\nu+1)} g(z^{-1}). \tag{20}$$

The control law of the unconstrained system for this modified rate limiter and plant becomes,

$$\begin{aligned} \tilde{w}_{\varphi_m}[k] &= -{\sigma_m}^{-1} q_m(z^{-1})\varphi(z^{-1})\rho(z^{-1})\hat{d}_m[k] \\ \hat{d}_m[k] &= \eta_m[k] - \sigma_m \tilde{g}(z^{-1}) \tilde{w}_{\varphi_m}[k]. \end{aligned} \tag{21}$$

Since $\tilde{w}_{\varphi_m}[k] = \rho(z^{-1})w_{\varphi_m}[k]$, from (19) and (21) it can be seen that $\tilde{w}_{\varphi_m}[k]$ is equivalent to $w_{\varphi_m}[k]$. Therefore $q_m(z^{-1})$ is designed for the modified system rate limiter and plant which gives the desired input $w_{\varphi_m}[k]$ for the real system. For

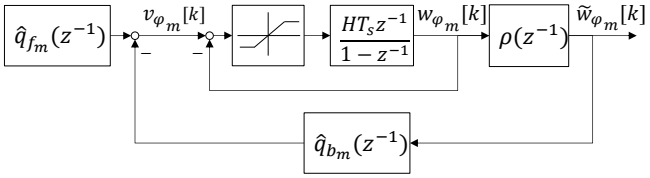

Fig. 2. Modified IMC structure for anti-windup

the IMC structure, $q_m(z^{-1})$ would normally be chosen as the approximate inverse of the plant dynamics [22], but because of the modified rate limiter, $q_m(z^{-1})$ is chosen as the pseudo inverse of $\tilde{g}(z^{-1})$. However from (20), the minimum-phase part of the plant dynamics remains the same, so that

$$q_m(z^{-1}) = \frac{1-\beta_m}{1-\beta_m z^{-1}} \frac{1-a_1 z^{-1}}{b_0+b_1} \tag{22}$$

with $\beta_m = e^{-\zeta_m T_s}$, where ζ_m is a tuning parameter that can be different for each mode and is discussed in [3], [11].

B. Anti-windup compensation

In [12], [14], it is stated that a better dynamic response is gained by including a feedback term around the non-linearity when the non-linear element is a saturation. In the previous section, $q_m(z^{-1})$ has been designed for the modified system which was demonstrated to be equivalent for the design of the original system. One way of achieving anti-windup capabilities with an IMC structure for saturating nonlinearities is by factorising $q_m(z^{-1})$ as

$$q_m(z^{-1}) = \left[1+q_{b_m}(z^{-1})\right]^{-1} q_{f_m}(z^{-1}) \tag{23}$$

when $q_{b_m}(z^{-1})$ is in the feedback loop around the saturation. Since there already exists a unity feedback loop in the rate limiter structure, there is a natural factorization given by

$$q_{f_m}(z^{-1}) = q_m(z^{-1}), \quad q_{b_m}(z^{-1}) \quad = \frac{z^{-1}}{1-z^{-1}}. \tag{24}$$

Therefore, $\bar{q}_m(z^{-1})$ can be defined such that

$$\begin{aligned} \bar{q}_m(z^{-1}) &= q_{f_m}(z^{-1}) \left[1+q_{b_m}(z^{-1})\right]^{-1} \\ &= (1-z^{-1}) q_m(z^{-1}) \end{aligned} \tag{25}$$

and can be factorised into $\bar{q}_{f_m}(z^{-1})$ and $\bar{q}_{b_m}(z^{-1})$, in order to tradeoff performance and robustness, where $\bar{q}_{b_m}(z^{-1})$ is still considered to be feedback around the saturation function only. Therefore the IMC anti-windup synthesis for saturating nonlinearities can be followed for the rate limiter. There are a number of approaches to parameterizing the IMC anti-windup. One factorisation choice is given in [14] where

$$\begin{aligned} \bar{q}_{f_m}(z^{-1}) &= \lambda \bar{q}(z^{-1}) + (1-\lambda)\bar{q}(0) \\ \bar{q}_{b_m}(z^{-1}) &= \bar{q}_{f_m}(z^{-1}) \left[\bar{q}(z^{-1})\right]^{-1} - 1. \end{aligned} \tag{26}$$

The choice of λ is discussed in [12] in detail. Another choice of parameterization be achieved via the coprime factorisation of the nominal plant or nominal controller such that the IMC anti-windup design is reduced to a convex search over the space of all right coprime factors of the linear plant [23], [24]. However for this paper, the factorisation in (26) is used to demonstrate the anti-windup design procedure.

Since the internal feedback loop of the rate limiter cannot be accessed physically, the structure in Fig. 2 is used i.e. the feedback controller is placed around the modified rate limiter. With the controllers selected in (26), by loop transformations, $\hat{q}_{f_m}(z^{-1})$ and $\hat{q}_{b_m}(z^{-1})$ can be defined for the structure in Fig. 2 where

$$\begin{aligned} \hat{q}_{f_m}(z^{-1}) &= \bar{q}_{f_m}(z^{-1}) \\ \hat{q}_{b_m}(z^{-1}) &= \left[(1-z^{-1})\bar{q}_{b_m}(z^{-1}) - z^{-1}\right]. \end{aligned} \tag{27}$$

The loop equations without anti-windup compensation can be written as

$$\begin{aligned} v_{\varphi_m}[k] &= -\sigma_m{}^{-1} q_m(z^{-1}) \mu_m[k] \\ \eta_m[k] &= \mu_m[k] \left[1 - \tilde{g}(z^{-1}) q_m(z^{-1})\right] \end{aligned} \tag{28}$$

so the controller acts only on the output disturbance. However if a feedback loop is included around the nonlinearity, then the controller output becomes

$$\begin{aligned} v_{\varphi_m}[k] &= -\sigma_m{}^{-1} \hat{q}_{f_m}(z^{-1}) \mu_m[k] - \hat{q}_{b_m}(z^{-1}) \tilde{w}_{\varphi_m}[k] \\ \eta_m[k] &= \mu_m[k] \left[1 - \tilde{g}(z^{-1}) \hat{q}_{f_m}(z^{-1})\right] \\ &\quad - \sigma_m \tilde{g}(z^{-1}) \hat{q}_{b_m}(z^{-1}) \tilde{w}_{\varphi_m}[k] \end{aligned} \tag{29}$$

so that the controller acts on the error signal as well as the effect of the rate limiter on the control action.

V. IQC ROBUST STABILITY ANALYSIS

To consider plant model mismatch, a norm-bounded operator $\mathbf{\Delta}_p \in \mathbb{C}^{M\times M}$ is introduced which represents an unknown additive perturbation to the nominal plant in modal space. The modal decomposition of the plant is then represented as

$$\mathbf{y}[k] = \mathbf{\Phi} \left[g(z^{-1})\mathbf{\Sigma} + \mathbf{\Delta}_p\right] \mathbf{\Psi}^{\mathrm{T}} \tag{30}$$

In practice, the main sources of uncertainty are in the spatial response, but for this paper, the general case of uncertainty in the dynamic response and the spatial response is considered. If $\mathbf{\Delta}_p$ is diagonal, it represents independent variations in each mode, but if $\mathbf{\Delta}_p$ is unstructured it represents uncertainties in the column and row spaces of $\mathbf{B}$ (i.e. actuator and sensor inaccuracies) and the process dynamics [25]. For stability analysis, the closed loop system is expressed in the standard feedback loop configuration depicted in [21]. The closed loop system is then completely characterized by

$$\mathbf{v}_\Delta[k] = \mathbf{R}(z^{-1}) \mathbf{w}_\Delta[k], \quad \mathbf{w}_\Delta[k] = \mathbf{\Delta} \mathbf{v}_\Delta[k] \tag{31}$$

where the operator $\mathbf{\Delta} = \mathrm{diag}\{\mathbf{\Delta}_\varphi, \mathbf{\Delta}_p\}$ encapsulates the rate limiter and the uncertainty in the closed loop such that,

$$\mathbf{v}_\Delta[k] = \begin{bmatrix} \mathbf{v}_\varphi[k] \\ \mathbf{v}_{\Delta_p}[k] \end{bmatrix}, \quad \mathbf{w}_\Delta[k] = \begin{bmatrix} \tilde{\mathbf{w}}_\varphi[k] \\ \mathbf{w}_{\Delta_p}[k] \end{bmatrix} \tag{32}$$

and $\mathbf{R}(z^{-1})$ is a linear time invariant (LTI) transfer matrix, which for the closed loop for each mode is given as,

$$\mathbf{R}(z^{-1}) = \begin{bmatrix} -\mathbf{Q}_b(z^{-1}) & -\mathbf{\Sigma}^{-1}\mathbf{Q}_f(z^{-1}) \\ \left[\rho(z^{-1})\right]^{-1}\mathbf{I} & \mathbf{0} \end{bmatrix}. \tag{33}$$

For mixed uncertainty, $\mathbf{\Delta}_p \in \mathrm{IQC}(\mathbf{\Pi}_{\Delta_p})$ and $\mathbf{\Delta}_\varphi \in \mathrm{IQC}(\mathbf{\Pi}_\varphi)$, where $\mathbf{\Pi}_p$ and $\mathbf{\Pi}_\varphi$ are chosen as in [19], [21] to model the uncertainties. If $\mathbf{R}(z^{-1})$ has the following state space representation $\mathbf{R}(z^{-1}) = \mathbf{C}_R(z^{-1}\mathbf{I} - \mathbf{A}_R)^{-1}\mathbf{B}_R + \mathbf{D}_R$ such that the pair $(\mathbf{A}_R, \mathbf{B}_R)$ is controllable and $\mathbf{A}_R$ has no eigenvalues on the imaginary axis, then the frequency domain characterization of the main IQC condition in [21] is that

$$\begin{bmatrix} \left(e^{j\omega}\mathbf{I} - \mathbf{A}_R\right)\mathbf{B}_R \\ \mathbf{I} \end{bmatrix}^* \mathbf{\Pi} \begin{bmatrix} \left(e^{j\omega}\mathbf{I} - \mathbf{A}_R\right)\mathbf{B}_R \\ \mathbf{I} \end{bmatrix} \leq -\varepsilon\mathbf{I}. \qquad (34)$$

By the discrete KYP Lemma [26], (34) is equivalent to satisfying the feasibility problem,

$$\mathbf{\Pi} + \begin{bmatrix} \mathbf{A}_R^{\mathrm{T}}\mathbf{X}\mathbf{A}_R - \mathbf{X} & \mathbf{A}_R^{\mathrm{T}}\mathbf{X}\mathbf{B}_R \\ \mathbf{B}_R^{\mathrm{T}}\mathbf{X}\mathbf{A}_R & \mathbf{B}_R^{\mathrm{T}}\mathbf{X}\mathbf{B}_R \end{bmatrix} \leq 0 \qquad (35)$$

such that there exists some matrix $\mathbf{X}^{\mathrm{T}} = \mathbf{X}$ where $\mathbf{\Pi}$ is structured as [25]

$$\mathbf{\Pi} = \begin{bmatrix} \mathbf{\Pi}_{11} & \mathbf{\Pi}_{12} \\ \mathbf{\Pi}_{21} & \mathbf{\Pi}_{22} \end{bmatrix} \qquad (36)$$

with

$$\begin{aligned} \mathbf{\Pi}_{11} &= \mathbf{C}_R^T \mathbf{\Pi}_{\Delta(11)} \mathbf{C}_R \\ \mathbf{\Pi}_{12} &= \mathbf{\Pi}_{21}^* = \mathbf{C}_R^{\mathrm{T}} \mathbf{\Pi}_{\Delta(12)} + \mathbf{C}_R^T \mathbf{\Pi}_{\Delta(11)} \mathbf{D}_R \\ \mathbf{\Pi}_{22} &= \mathbf{\Pi}_{\Delta(22)} + \mathbf{\Pi}_{\Delta(21)} \mathbf{D}_R + \mathbf{D}_R^{\mathrm{T}} \mathbf{\Pi}_{\Delta(12)} + \mathbf{D}_R^{\mathrm{T}} \mathbf{\Pi}_{\Delta(11)} \mathbf{D}_R \end{aligned} \qquad (37)$$

and $\mathbf{\Delta} \in \mathrm{IQC}(\mathbf{\Pi}_{\mathbf{\Delta}})$ so that the uncertainties and rate limiter can be modeled with a convex combination of multipliers [27], such that $\mathbf{\Pi}_{\mathbf{\Delta}} = \mathrm{daug}\{\mathbf{\Pi}_\varphi, \mathbf{\Pi}_{\Delta_p}\}$ where $\mathrm{daug}(\cdot)$ represents the diagonal augmentation of the submultipliers described in [28].

VI. Case Study: Diamond Storage Ring

The feedback system at Diamond takes the beam position from 172 BPMs and calculates offsets to 172 corrector magnet power supplies, in each plane, at a rate of 10kHz. The requirement on the vertical positioning of the electron beam is particularly tight because the beam has an elliptical cross-section with the height being much smaller than the width. Therefore in this paper, the controller design for the vertical plane is presented. The process model in the form of (2) with $\nu = 7$, $T_s = 100\mu$s and $a = 700$rad.s^{-1} is given by

$$g(z^{-1}) = z^{-7} \frac{0.3558 z^{-1}}{1 - 0.6442 z^{-1}}. \qquad (38)$$

The controller in (22) can be designed by selecting a different β_m for each mode. However for the Diamond Storage Ring controller, a common β is used on all modes and the bandwidth of each mode is adjusted by a different gain s_m is applied to each mode. The controller dynamics for each mode, $q_m(z^{-1})$ is chosen with $\beta = e^{-T_s/\tau_d}$ so that,

$$\frac{s_m}{\sigma_m} q_m(z^{-1}) = \frac{s_m}{\sigma_m} \frac{0.3741 - 0.241 z^{-1}}{1 - 0.8669 z^{-1}} \qquad (39)$$

with $s_m = \sigma_m^2/(\sigma_m^2 + \delta)$ where, for this case, $\delta = 1$. For the IMC anti-windup design, the choice of λ in (26) is used to trade-off performance and stability [12]. Following from (27), where $\lambda = 0$ is chosen,

$$\hat{q}_{f_m}(z^{-1}) = 0.3741, \quad \hat{q}_{b_m}(z^{-1}) = \frac{-0.2227 z^{-1}}{1 - 0.6442 z^{-1}}. \qquad (40)$$

This choice of λ is generally expected to offer good compensation against input constraints but stability is not guaranteed. Using the test in (35), the robust stability of the system given in (40) can be determined. A structured uncertainty description is used so that the IQC in (37) can be described by

$$\mathbf{\Pi}_{\Delta(11)} = \begin{bmatrix} 2I & 0 \\ 0 & \gamma_{\Delta_p} I \end{bmatrix}, \quad \mathbf{\Pi}_{\Delta(22)} = \begin{bmatrix} -I & 0 \\ 0 & -\gamma_{\Delta_p} I \end{bmatrix} \qquad (41)$$

where γ_{Δ_p} is he upper bound of energy gain of the uncertainty. Fig. 3 shows how γ_{Δ_p} varies with each spatial mode for constrained IMC structure without feedback with the controller selected in (39) and with anti-windup structure with the controller selected in (40). Both systems are found to be stable for all modes, although the size of the allowable uncertainty for the anti-windup design is less than that of the constrained conventional IMC structure. On the other hand, using $\lambda = 1$ results in the conventional IMC structure for which nominal stability is guaranteed [22], however the performance may be sluggish. Fig. 4 shows the integrated beam displacement of the IMC controller without anti-windup is compared to that with anti-windup where $\lambda = 0$. At 100Hz the RMS deviation of the uncontrolled beam is 0.6μm (i.e. 10% beam size) and with feedback control (unconstrained) the RMS deviation is 0.3μm (i.e. 5% beam size). At frequencies above 200Hz, the effect of rate limiter can be seen. It is shown that when the system is constrained, the IMC anti-windup structure is able to suppress disturbances to a greater extent at higher frequencies, where the effect of the rate limiter is greatest, compared to the constrained system without the anti-windup feedback loop. It should be noted however that choosing $\lambda = 0$ does not necessarily correspond to the optimal achievable constrained performance.

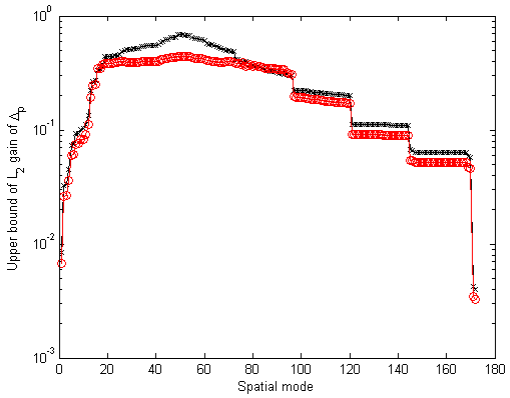

Fig. 3. Upper bound of L_2 gain of additive uncertainty Δ_p for the rate constrained system without anti-windup ('x-' black plot) and for rate constrained system with anti-windup where $\lambda = 0$ ('o-' red plot) and for a rate limit of 1.5A/s

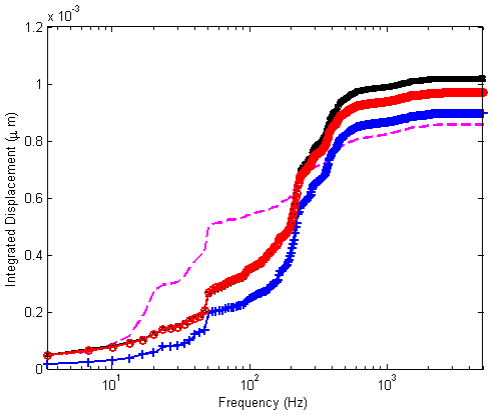

Fig. 4. Uncontrolled integrated beam motion at first vertical BPM ('- -' magenta) and controlled integrated beam motion for the unconstrained system ('+-' blue), the rate constrained system with no anti-windup ('x-' black) and rate constrained system with anti-windup where $\lambda = 0$ ('o-' red plot) and for a rate limit of 1.5A/s

VII. CONCLUSIONS

This paper has considered anti-windup synthesis based on IMC for rate constrained actuators for electron beam stabilisation control systems of synchrotrons. The common practice of factorising the unconstrained IMC controller to include a feedback term around a nonlinearity to improve constrained performance is not straightforward for rate limiters that are implemented with an internal feedback path. The method in [19] is used which includes a first order filter after the rate limiter to ensure the L_2 stability of the rate limiter. By including a corresponding filter at the input to the plant, an unconstrained IMC controller can then be designed for this modified rate limit and plant. The IMC structure is utilised to give anti-windup capabilities by first modifying the standard IMC structure to include feedback around the saturation only and by loop transformations, define the feedback term to include the entire rate limiter. This ensures that the anti-windup factorisations are strictly proper. It was shown that this structure can provide improved performance over the standard IMC structure when the actuators are constrained and furthermore that the system is guaranteed stable in the presence of input rate constraints. Robust analysis results and simulation results of the performance for the Diamond Storage Ring system under rate constraints have been presented.

ACKNOWLEDGMENT

The authors would like to thank Diamond Light Source for supporting this work.

REFERENCES

[1] R. Bartolini, "The commissioning of the Diamond Storage Ring," in *22nd Particle Accelerator Conf.*, Albuquerque, New Mexico, 2007.

[2] N. Hubert, L. Cassinari, J.-C. Denard, A. Nadji, and L. Nadolski, "Global orbit feedback systems down to DC using fast and slow correctors," in *9th European Workshop on Beam Diagnostics and Instrumentation for Particle Accelerators*, Basel, Switzerland, 2009.

[3] A. Napier, S. Gayadeen, and S. R. Duncan, "Fast orbit beam stabilisation for a synchrotron," in *IEEE Int. Conf. on Control Applicat.*, vol. 47, Denver, CO, 2011, pp. 1770–1775.

[4] J. Rowland, M. Abbott, J. Dobbing, M. Heron, I. Martin, G. Rehm, and I. Uzun, "Status of the Diamond fast orbit feedback system," in *Int. Conf. on Accelerator and Large Experimental Physics Control Systems*, Knoxville, Tennessee, 2007.

[5] G. Goodwin, B. Carny, and W. Edwards, "Analysis of thermal camber control in rolling mills," in *Proc. of the IFAC World Congr.*, Tallinn, USSR, 1990, pp. 160–164.

[6] S. R. Duncan, "The design of robust cross-directional control systems for paper making," in *Proc. of the American Control Conf. 1995*, vol. 3, Seattle, WA, 1995, pp. 1800 –1805.

[7] W. P. Heath, "Orthogonal functions for cross-directional control of web forming processes," *Automatica*, vol. 32, no. 2, pp. 183–198, 1996.

[8] S. R. Duncan and G. Bryant, "The spatial bandwidth of cross-directional control systems for web processes," *Automatica*, vol. 33, no. 2, pp. 139–153, 1997.

[9] P. E. Wellstead, M. B. Zarrop, and S. R. Duncan, "Signal processing and control paradigms for industrial web and sheet manufacturing," *Intl. J. Adaptive Control and Signal Processing*, vol. 14, no. 1, pp. 51–76, 2000.

[10] R. J. Steinhagen, "Real-time feedback on beam parameters," prepared for APAC 2007: Asian Particle Accelerator Conference, Indore, India, 29 Jan - 2 Feb 2007.

[11] S. R. Duncan, "The design of a fast orbit beam stabilisation system for the Diamond synchrotron," Dept. of Eng. Sci., University of Oxford, Tech. Rep. 2296/07, 2007.

[12] A. Zheng, M. V. Kothare, and M. Morari, "Anti-windup design for internal model control," *International Journal of Control*, vol. 60, pp. 1015–1024, 1993.

[13] G. Goodwin, S. Graebe, and W. Levine, "Internal model control of linear systems with saturating actuators," in *Proc. of the European Control Conference*, Groningen, 1993, pp. 1072–1077.

[14] W. P. Heath and A. G. Wills, "Design of cross-directional controllers with optimal steady state performance," *Eur. J. Control*, vol. 10, pp. 15–27, 2004.

[15] L. Rundqwist and K. Stahl-Gunnarsson, "Phase compensation of rate limiters in unstable aircraft," in *Control Applications, 1996., Proceedings of the 1996 IEEE International Conference on*, sep 1996, pp. 19 –24.

[16] J. Sofrony, M. C. Turner, and I. Postlethwaite, "Anti-windup synthesis for systems with rate-limits using riccati equations," *International Journal of Control*, vol. 83, no. 2, pp. 233–245, 2010.

[17] O. Brieger, M. Kerr, D. Leissling, I. Postlethwaite, J. Sofrony, and M. Turner, "Anti-windup compensation of rate saturation in an experimental aircraft," in *American Control Conference, 2007. ACC '07*, july 2007, pp. 924 –929.

[18] J. Sofrony, M. Turner, and I. Postlethwaite, "A simple anti-windup compensation scheme for systems with rate-limited actuators," in *ICCAS-SICE, 2009*, aug. 2009, pp. 3311 –3316.

[19] A. Megretski, "New IQC for quasi-concave nonlinearities," *Int. J. Robust and Nonlinear Control*, vol. 11, no. 7, pp. 603–620, 2001.

[20] E. Courant and H. Snyder, "Theory of the alternating gradient synchrotron," *Ann. Physics*, vol. 3, pp. 1–48, 1958.

[21] A. Megretski, "System analysis via Integral Quadratic Constraints," *IEEE Trans. Autom. Control*, vol. 42, no. 6, pp. 819–830, 1997.

[22] M. Morari and E. Zafiriou, *Robust Process Control*. Englewood Cliffs, NJ: Prentice-Hall, 1989.

[23] M. Turner, G. Herrmann, and I. Postlethwaite, "Incorporating robustness requirements into antiwindup design," *Automatic Control, IEEE Transactions on*, vol. 52, no. 10, pp. 1842 –1855, oct. 2007.

[24] A. Adegbege, "Constrained internal model control," Ph.D. dissertation, School of Electrical and Electronic Engineering, University of Manchester, 2011.

[25] R. Morales and W. Heath, "The robustness and design of constrained cross-directional control via Integral Quadratic Constraints," *IEEE Trans. Control Syst. Technol.*, vol. 19, pp. 1421–1432, Nov. 2011.

[26] A. Rantzer, "On the Kalman Yakubovich Popov lemma," *Syst. Control Lett.*, vol. 28, no. 1, pp. 7–10, 1996.

[27] U. Jonsson, "Lecture notes on integral quadratic constraints," 2001. [Online]. Available: http://www.math.kth.se/ uj/Publications/publications.html

[28] L. El Ghaoui and S. Niculescu, Eds., *Advances in Linear Matrix Inequality Methods in Control: Advances in Design and Control*. Philadelphia, PA: SIAM, 2000.